HOKKAIDO UNIVERSITY

Title	In-Out Intermittency in Gap Junction-Coupled Class I^* Neurons
Author(s)	Tadokoro, Satoru; Yamaguchi, Yutaka; Tsuda, Ichiro et al.
Citation	Hokkaido University Preprint Series in Mathematics, 762, 1-16
Issue Date	2005
DOI	https://doi.org/10.14943/83912
Doc URL	https://hdl.handle.net/2115/69570
Type	departmental bulletin paper
File Information	re762.pdf

Hokkaido University Collection of Scholarly and Academic Papers : HUSCAP

In-Out Intermittency in Gap Junction-Coupled Class I^* Neurons

Satoru Tadokoro,[1,*] Yutaka Yamaguti,[1] Ichiro Tsuda,[2,1] and Hiroshi Fujii[3]

[1]*Department of Mathematics, Graduate School of Science,*
Hokkaido University, Sapporo 060-0810, Japan

[2]*Laboratory of Computational Life Science,*
Research Institute of Electronic Science,
Hokkaido University, Sapporo 060-0812, Japan

[3]*Department of Information and Communication Sciences,*
Kyoto Sangyo University, Kyoto 603-8555, Japan

Abstract

In a series of papers, we have proposed a dynamical model for gap junction-coupled networks of class I^* neurons, and investigated its dynamic characters. We found various dynamic states in a model neural network with diffusively coupled class I^* neuron models, called μ-models. Among others, hierarchies of intermittent transitions attracted attention in relation with real brain dynamics. This paper is devoted to report a mechanism of the first transition appeared in the intermittenly transitory dynamics among an all-synchronized state, various metachronal waves and a weakly chaotic state. We clarify that this intermittent transition is described as an in-out intermittency.

*Electronic address: tadokoro@math.sci.hokudai.ac.jp

We studied a network of a certain kind of model of neuron one-dimensionally coupled by a diffusion-type coupling. We found that the network exhibits an intermittently transitory behavior among three kinds of states: almost all-synchronized state, various metachronal waves, and a weakly chaotic state. A metachronal wave means a wave with orderly phase shifts of neurons' activity and is observed in the movement of insects like a centipede. Our network has an invariant subspace resulting from a mirror symmetry with respect to neurons' indices. This transitory behavior is intermittency in the form of trajectories intermittently approaching and leaving the mirror symmetric invariant subspace. We found that the intersection of the attractor of this intermittency and the invariant subspace is not a minimal attractor but contains two invariant sets: the all-synchronized state and a symmetric metachronal wave. The former is tranversely repelling to the invariant subspace whereas the latter is transeversely attracting. These natures of transversal stabilities of the invariant sets induce approaching and leaving the invariant subspace: The all-synchronized state and the symmetric metachronal wave give rise to the leaving phase (out-phase) and the approaching phase (in-phase), respectively. In the invariant subspace, the weakly chaotic state and the other symmetric metachronal waves make two different pathways from the symmetric metachronal wave to the all-synchronized state. According to Ashwin, if the intersection of an intermittent attractor in the above sense and its relating invariant subspace is a minimal attractor, then it is on-off intermittency, whereas if the intersection is not necessarily a minimal attractor, it is in-out intermittency. Therefore, the dynamical mechanism of the intermittently transitory behavior in our network is in-out intermittency. This transitory behavior attracts attention as a possible mechanism describing the nonstationary and transitory phenomena observed experimentally in the mammalian neocortex.

I. INTRODUCTION

Gap junction couplings, i.e, electric couplings among certain kinds of interneurons, such as first spiking (FS) and low threshold spiking (LTS) interneurons are recently discovered to exist ubiquitously in the mammalian neocortex. It is also known that neurons are classified into two classes called class I and class II depending on the difference of a set of effective ion channels. A typical class I model neuron is a Connor type of neuron, and a typical class II model neuron is a Hodgkin-Huxley type of neuron. Now it is generally recognized that

most of cortical neurons belong to class I[2].

In our previous studies[3–5], we have defined a subclass of class I neurons, which we called a class I^*, by the following three characteristics: 1. the presence of limit cycles whose periods tend to infinity in the limit of a saddle-node bifurcation; 2. the presence of a narrow channel made of two nullclines expressing the steady state condition of the dynamical system; 3. the presence of a fixed point to be an unstable spiral. We investigated dynamical behaviors of a network consisting of the class I^* neurons, coupled by gap junctions. Then we found that they exhibited transitory behaviors among various dynamical states. Such transitory behaviors were proposed as describing the nonstationary and transitory phenomena observed experimentally in the mammalian neocortex[6]. Thus it is worth studying the mechanism of such transitory behaviors in both aspects of the dynamical systems and of the neuroscience.

Among the transitory behaviors that our model networks exhibit, we here focus on the dynamical behavior consisting of three dynamical components of an almost synchronized state, metachronal waves and a weakly chaotic state. Here a metachronal wave means a wave with orderly phase shifts of neurons' activity. This transition is the first transiton of hierarchical transitions which the networks exhibit along with the variation of the gap junction coupling strength. In the second transition, another dynamical component which is strongly chaotic appears.

In the present paper, we show that the dynamical mechanism of the first transition is in-out intermittency[7].

II. μ-MODEL AND THEIR GAP JUNCTION-COUPLED NETWORK

We use μ-model[3], a simple model which possesses minimal features to express class I^* neurons. The μ-model is a two-valiable model where the first variable V represents the membrane potential of neuron, the second one R is a recovery variable representing an activation state in a general sense. Equations for the model can be as follows:

$$\begin{cases} \frac{dV}{dt} = -R - \mu V^2(V - \frac{3}{2}) + I \\ \frac{dR}{dt} = -R + \mu V^2 \end{cases} \tag{1}$$

where I is the strength of an injected current which we view as a bifurcation parameter, and μ can also be a bifurcation parameter, but it will be fixed to the value, 1.65 through

this paper.

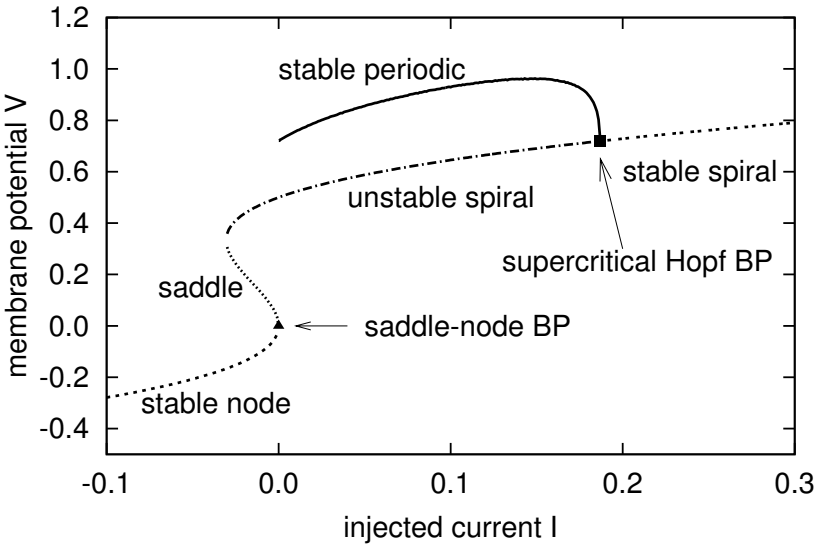

FIG. 1: Bifurcation diagram of μ-mudel. For stable periodic states, maximum values of the membrane potential are plotted.

This model exhibits saddle-node and Hopf bifucations. The bifurcation diagram of the model is shown in Fig.1. Action potentials are plotted in Fig.2(a) for $I = 0.004$. A corresponding trajectory and nullclines are shown in Fig.2(b).

We use a diffusion-type coupling as a model of the gap junction [8]. We adopt a free boundary condition, in correspondence with the Neumann type of boundary conditon in the continuous space limit. The model network used here is as follows:

$$\begin{cases} \frac{dV_i}{dt} &= -R_i - \mu V_i^2(x - \frac{3}{2}) + I + J_i \\ \frac{dR_i}{dt} &= -R_i + \mu V_i^2 \end{cases} \tag{2}$$

$$J_i = \begin{cases} g(V_2 - V_1) & (i = 1) \\ g(V_{i+1} + V_{i-1} - 2V_i) & (i = 2, ..., N-1) \\ g(V_{N-1} - V_N) & (i = N) \end{cases} \tag{3}$$

Hereafter, we fixed the number of neurons N to 16 and the injected current I to 0.004, where, together with appropriate coupling strengths, a typical intermittent transition can occur.

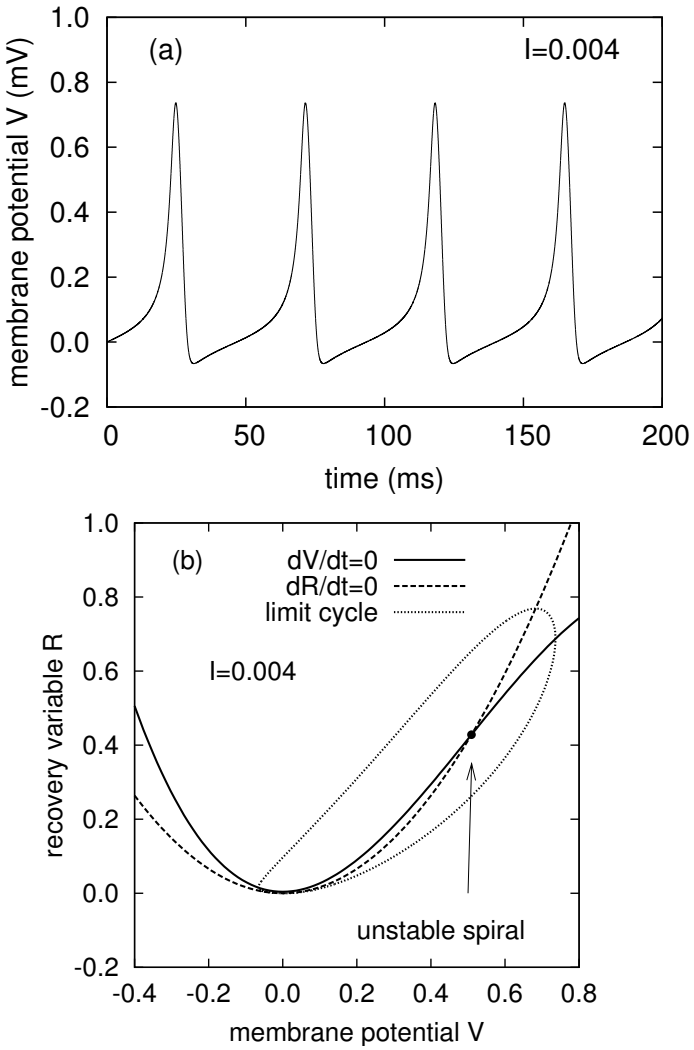

FIG. 2: (a) Action potentials and (b) a corresponding trajectory and nullclines.

III. TRANSITORY BEHAVIORS AMONG A SYNCHRONIZED STATE, METACHRONAL WAVES AND A WEAKLY CHAOTIC STATE

Figure 3 shows a spatio-temporal contour map of the amplitude of V-variables of 16 μ-model neurons coupled with the strength, $g = 0.255$. As shown in the figure, characteristic spatiotemporal patterns appear, corresponding to some dynamic states and gradual transitions between them.

One can identify six kinds of patterns as follows. A pattern representing an almost synchronized state appears around $t \sim 51800$ and also during $t \sim 53400 - 54200$. A pat-

tern appearing during $t \sim 52600 - 53400$ is identified to be a chaotic state which is very weak chaos. Hereafter we refer this state as a weakly chaotic state. There appear various metachronal wave patterns, which can be classified into four kinds of patterns, according to whether or not they preserve spatial symmetries with respect to neurons' indices, and also according to whether or not they are rapidly modulated as time progresses: a symmetric one appearing during $t \sim 52400 - 52600$ and $t \sim 54900 - 55900$, modulated symmetric one appearing during $t \sim 55900 - 56600$, two different modulated asymmetric ones appearing during $t \sim 52100 - 52400$ and $t \sim 54200 - 54600$.

It is not so easy to identify temporal boundaries of these patterns only by observing such a contour map, as is shown in Fig.3, because transitions between the patterns are very slow and look continuous. Nevertheless, a Poincaré map which will be mentioned below (Fig.4) makes these identification easy.

Because a single μ-model neuron exhibits a limit cycle oscillation under the above conditions, the introduction of a coordinate such as eliminating this periodic component should make the essential structure clarify. For this purpose, a Poincaré section transversally set up to the limit cycle is useful.

Actually we found an appropriate Poincaré map for extracting the embedded dynamical structure in the time series such as shown in Fig3, using a Poincaré section of $\sum_{i=1}^{N} V_i/N = 0.2$. The projection to the (V_1, V_8) plane of the Poincaré map on the section is shown in Fig.4(a). An attractor representing the transitions between the dynamical states is clearly visible on this Poincaré section. We estimated the largest Lyapunov exponent of this attractor, using the standard method[15, 16], which is about 0.001635. Thus this attractor is a chaotic attractor.

Figure 4(b) shows correspondence between dynamical states and the parts of the attractor on the section. Two saddles at $(V_1, V_8) = (0.2, 0.2)$ and $\sim (0.15, 0.25)$ in Fig.4(a) are denoted by AS and SMW respectively in Fig.4(b). The former corresponds to an all-synchronized state in which all neurons are synchronized. Spatio-temporal patterns around $t \sim 51800$ and during $t \sim 53400 - 54200$ in Fig3 correpond to AS. The latter corresponds to a state which exhibits the symmetric metachronal wave pattern such as appears during $t \sim 52400 - 52600$ and $t \sim 54900 - 55900$ in Fig.3.

Two kinds of trajectories from AS to SMW represent modulated asymmetric metachronal waves denoted by $MAMW$. Such spatio-temporal patterns appearing during

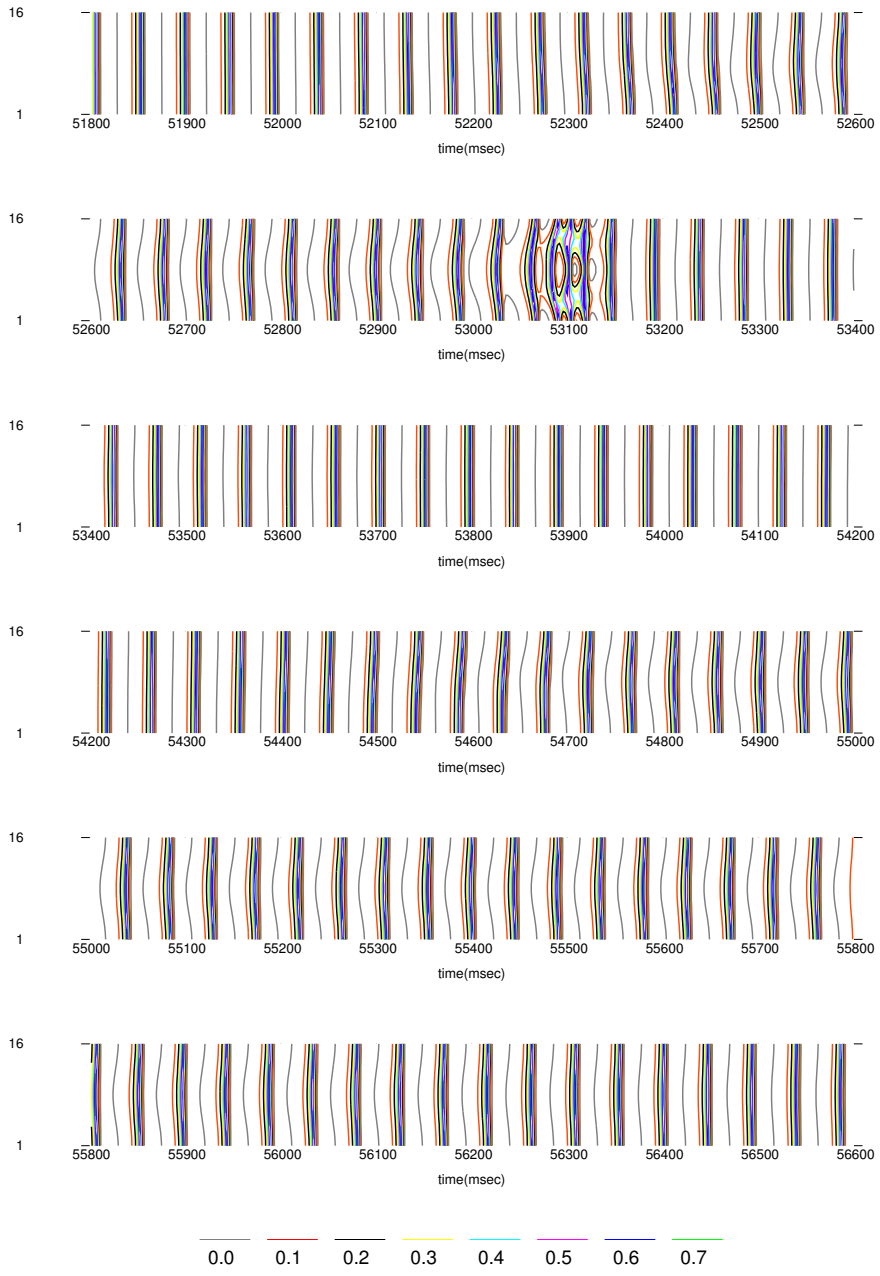

FIG. 3: Spatio-temporal patterns represented by a contour map. Color denotes the level of amplitude of the V-variable (the membrane potential). $N = 16$, $\mu = 1.65$, $I = 0.004$, $g = 0.255$.

$t \sim 52100 - 52400$ and $t \sim 54200 - 54600$ in Fig.3 correspond to the right and left curves, respectively, denoted by $MAMW$ in Fig.4(b). A straight-like line from SMW to AS represents modulated symmetric metachronal waves like a spatio-temporal pattern appearing during $t \sim 55900 - 56600$ in Fig.3. Trajectories starting from the SMW, experiencing

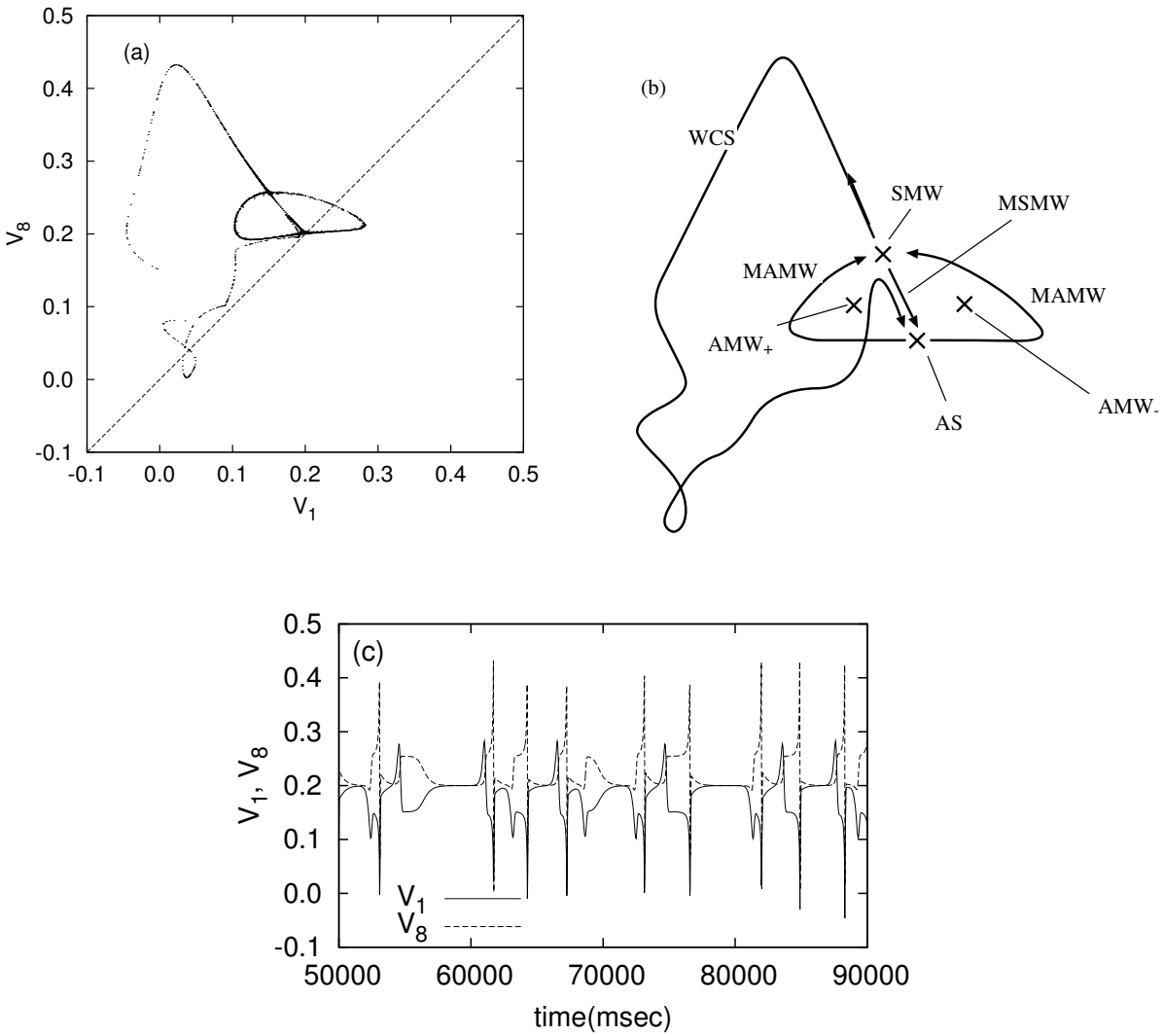

FIG. 4: A Poincaré map for $I = 0.004$, $g = 0.255$. (a) The projection to the (V_1, V_8) plane of the Poincaré map with the Poincaré section of $\sum_{i=1}^{N} V_i/N = 0.2$. (b) Correspondence between the parts of an attractor on the Poincaré section and dynamic states. (c) Time series of the voltages of the first and the 8-th neurons. Here time is in discrete time steps, which measures a trajectory on the Poincaré section.

a large excursion and coming back to the AS, represents the weakly chaotic state, which appears as patterns of $t \sim 52600 - 53400$ in Fig.3. We denoted the weakly chaotic state by WCS. In Fig.4(b), two asymmetric metachronal waves which are not modulated are denoted by ASM_+ and ASM_-. They do not appear in Fig.4(a) because they are unstable periodic states.

Figure 4(c) shows the time series of the voltage of the first and the 8-th neurons on the Poincaré section. One can see persistence of the all-synchronized state and the symmetric metachronal wave and the transitions between the modulated metachronal waves and the weakly chaotic state through these two saddles.

A little decrease in the coupling strength ($g \sim 0.248$) results in instability of this attractor and its change to a attractor ruin, and causes intermittent transitions between the attractor ruin and strong chaos, which is not described here. We interpreted this transition as a chaotic itinerancy[10–14] in another paper[3]. A typical example of this itinerant transition for $N = 30$ case and the discussion about it should be referred to Ref.[3].

In the next section, we investigate the dynamics of the attractor shown in Fig.4 in detail.

IV. IN-OUT INTERMITTENCY

Our model has an invariant subspace derived from a mirror symmetry with respect to neurons' indices, such as

$$V_i = V_{N-i+1}, \quad R_i = R_{N-i+1}, \quad i = 1, ..., N/2 \quad (N = even), \tag{4}$$

$$V_i = V_{N-i+1}, \quad R_i = R_{N-i+1}, \quad i = 1, ..., (N-1)/2 \quad (N = odd). \tag{5}$$

The all-synchronized state, the symmetric metachronal waves, and the weakly chaotic state belong to this invariant subspace, whereas the modulated asymmetric metachronal waves are outside the subspace.

Figure 5 shows a time series of distance from the invariant subspace for this dynamic behavior. In this figure, we can see intermittent behaviors: the presence of trajectories intermittently approaching and leaving the invariant subspace. It turns out that this intermittency is not on-off intermittency but in-out intermittency[7], because the intersection of this attractor and the invariant subspace is not a minimal attractor, but contains at least two invariant sets, which are the all-synchronized state, and the symmetric metachronal wave.

Comparison between Fig.5 and Fig.4c shows that the increase and the decrease of the distance occur when (V_1, V_8) is close to $(0.2, 0.2)$ representing the all-synchronized state and $(0.15, 0.25)$ representing the symmetric metachronal wave, respectively. Therefore, the all-

synchronized state is transversely repelling to the subspace, giving rise to the "out-phase", whereas the symmetric metachronal wave is transversely attracting, giving rise to the "in-phase". We calculated the largest normal Lyapunov exponent of the all-synchronized state, using the method of ref.[15, 16]. It is about 0.007, which is consistent with the growth rates roughly estimated by using the data of Fig.5. Concerning the stability within the subspace, the all-synchronized state is attracting, whereas the symmetric metachronal waves state is repelling.

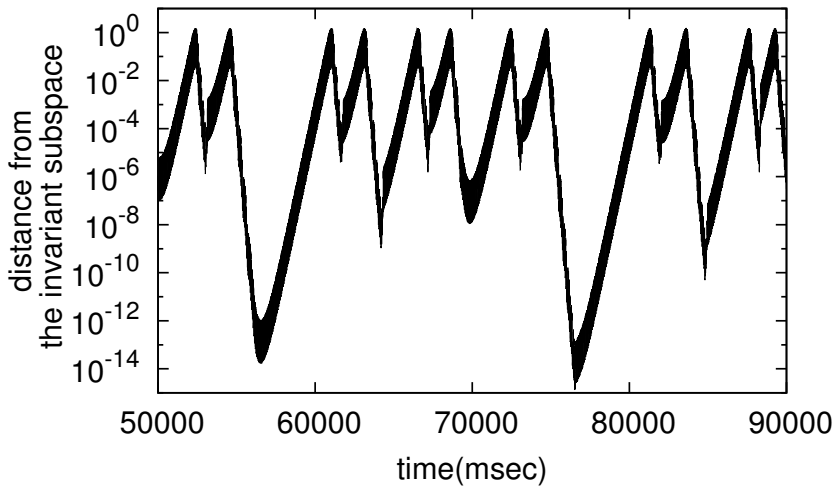

FIG. 5: Time series of distance from the invariant subspace on the logarithmic scale during the same period as in Fig.4c.

Within the subspace, there are two pathways from the symmetric metachronal wave to the all-synchronized state. One is through the weakly chaotic state and the other is through the modulated symmetric metachronal waves.

Therefore, the scenario of the intermittency is sketched as follows. A trajectory approaches the symmetric metachronal wave on the invariant subspace, and then close to the all-synchronized state via the weakly chaotic state or the modulated symmetric metachronal waves. After the trajectory stays for some time in the neighborhood of the invariant subspace, it leaves there with the form of the modulated asymmetric metachronal waves. A schematic representation of this scenario is depicted in Fig.6.

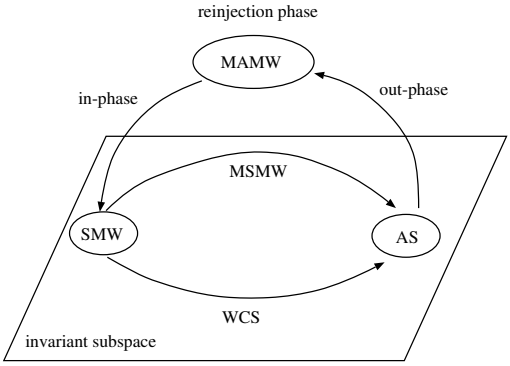

FIG. 6: Schematic diagram showing elements of the intermittent chaos shown in Fig.4.

V. PRODUCTION MECHANISM OF THE WEAKLY CHAOTIC PATHWAY

We discuss about production mechanism of the weakly chaotic pathway from the symmetric metachronal wave to the all-synchronized state. Discussion about the production mechanism of the eight-shaped part of this attractor should be referd to Ref.[3]

In the invariant subspace, it is a chaotic transient (transient chaos) and finally asymptotes the all-synchronized state. For $g \geq 0.31$, we found a chaotic attractor which is similar as a spatio-temporal pattern to the chaotic transient. It exhibits repeatedly spatio-temoral patterns similar to the pattern appearing during $t \sim 52600 - 53400$ in Fig3. Figure.7a shows the Poincaé map of this chaotic attractor for $g = 0.31$. The largest tangential and normal Lyapunov exponent of this attractor are 0.01033 and -0.00728, respectively.

The vanishing of the chaotic attractor for $g < 0.31$ results from a crisis: a contact of a stable manifold of the symmetric metachronal wave with the basin boundary of the chaotic attractor. In the invariant subspace, this crisis can be considered to be a boundary crisis[17] because it casuses sudden destruction of the chaotic attractor. For g values which are less than 0.31 and close to 0.31, some of trajectories starting from the neighborhood of the symmetric metachronal wave spend several cycles on the chaotic transient of what was the chaotic attractor at $g \geq 0.31$ before escaping and converging to the all-synchronized state as shown in Fig.7b. Here we call approximate times which it takes for a trajectory starting from the vicinity of the symmetric metachronal wave to come back via the chaotic transient, a cycle of the weakly chaotic orbit. One spatio-temporal pattern similar to the pattern appearing during $t \sim 52600 - 53400$ in Fig.3 corresponds to one cycle of the weakly chaotic orbit. Figure 7b suggests possibility that there exists an underlying chaotic saddle which the

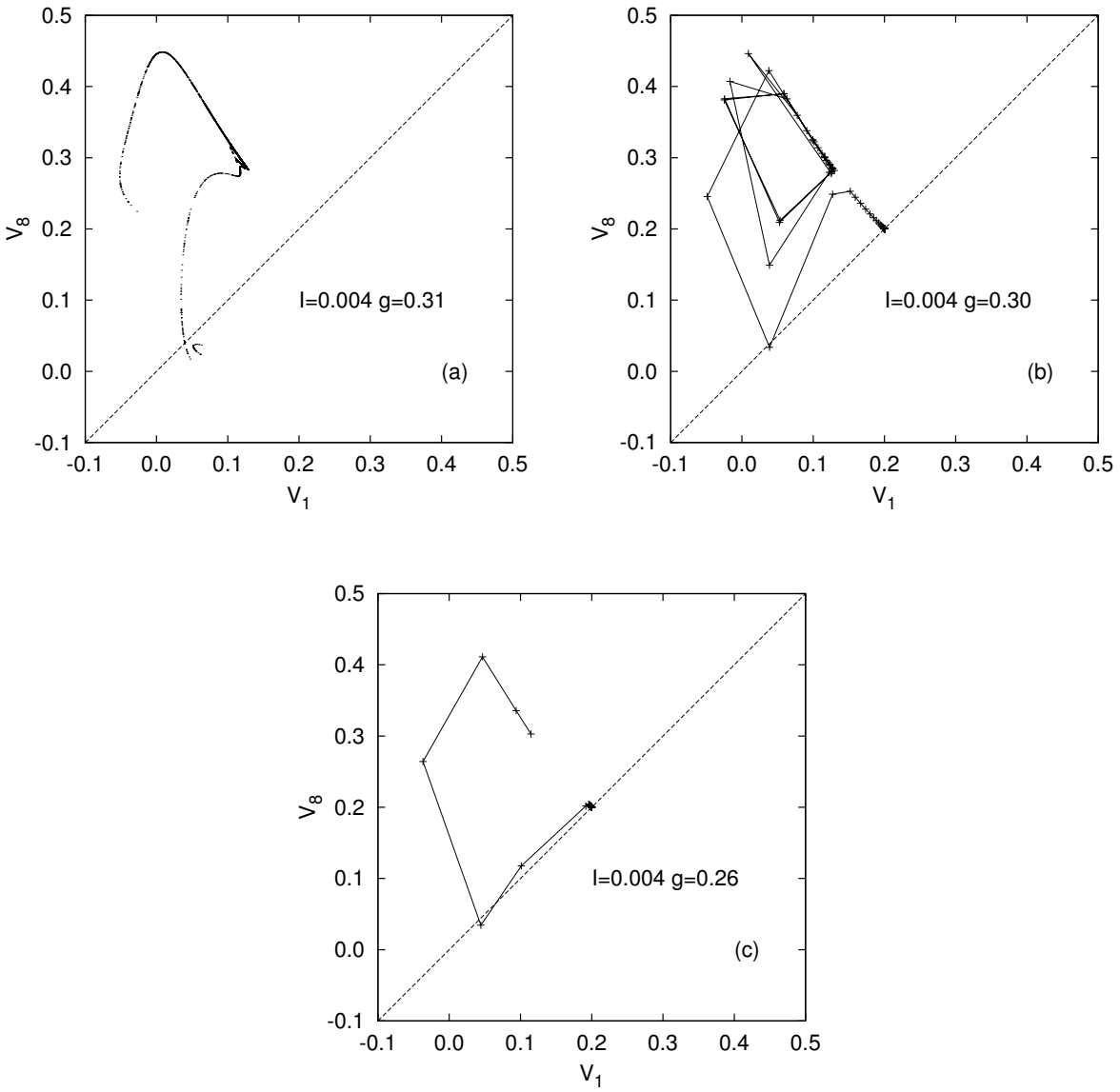

FIG. 7: Poincaré maps of weakly chaotic states in the invariant subspace. (a) A chaotic attractor for $I = 0.004$, $g = 0.31$. (b) A chaotic transient for $I = 0.004$, $g = 0.30$. Points on a trajectory are denoted by cross and are connected with lines. (c) A chaotic transient for $I = 0.004$, $g = 0.260$.

chaotic attractor converts to. Nevertheless it seems that this chaotic saddle disappears at $g \sim 0.29$, because trajectories entering the weakly chaotic orbit after only one cycle rapidly fall into the all-synchronized state as shown in Fig.7c.

For $0.258 < g < 0.31$, once a trajectory visits the all-synchronized state, it never visits the weakly chaotic state again, because a gateway from the modulated metachronal waves to

the weakly chaotic state does not exist. Therefore, there does not appear the coresponding part to the weakly chaotic state on the Poincaré section. For example, for $g \sim 0.26$, there appears only an eight-shaped attractor which consists of the all-synchronized state and the modulated metachronal waves on the section (see Fig.8).

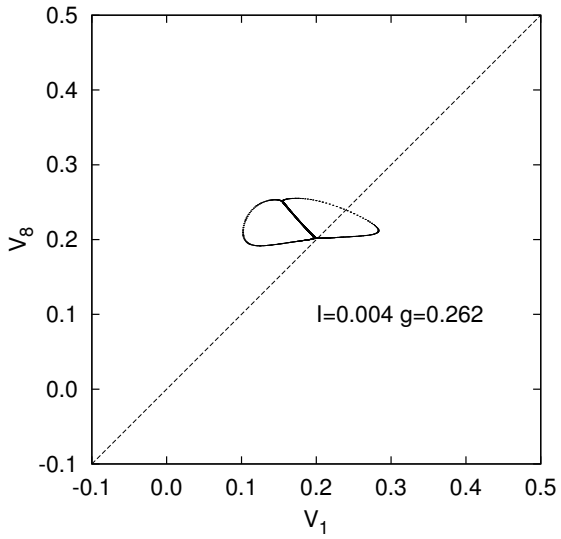

FIG. 8: A Poincaré map of an eight-shaped attractor. $I = 0.004$, $g = 0.26$.

A little more decrease in the coupling strength from $g \sim 0.26$ causes a collision between an stable manifold of the symmetric metachronal wave and the boundary of attracting region of the eight-shaped attractor, and consequently it makes a gateway to the weakly chaotic state in the vicinity of the symmetric metachronal wave. Therefore, a trajectory can visit the weakly chaotic state again and again.

VI. SUMMARY AND DISCUSSIONS

We found an in-out intermittency in the network of class I^* neurons, which is a one-dimensionally coupled network by gap junctions. This network possesses an invariant subspace stemming from the mirror symmetry with respect to neurons' indices. In this invariant subspace, there are two invariant sets: The all-synchronized state, the symmetric metachronal wave. The first one is transversely unstable and attracting in the invariant subspace. The second one is transversely stable and repelling in the subspace. The all-

synchronized state and the symmetric metachronal wave cause in-phase and out-phase of in-out intermittency, respectively. In the subspace there are two pathways from the symmetric metachronal wave to the all-synchronized state. One is the modulated symmetric metachronal waves and the other is the weakly chaotic state. The latter comes from a ghost of what is the chaotic attractor at $g > 0.31$. The two different modulated asymmetric metachronal waves constitute the nonlinear reinjection phase.

We mention about the case of other injected current strengths. For example, in the case of $I = 0.005$, we found a similar in-out intermittency at $g = 0.298$ in a Poincaré map to the in-out intermittency for $I = 0.004$ and $g = 0.255$. Neveretheless, These are different from each other: In the in-out intermittency for $I = 0.005$ and $g = 0.298$, trajectories entering the weakly chaotic orbit stay on it for several cycle before asymptoting the all-synchronized state, while in the intermittency for $I = 0.004$ and $g = 0.255$ trajectories entering the weakly chaotic orbit leave it after only one cycle. In the case of the in-out intermittency for $I = 0.005$ and $g = 0.298$, therefore, the chaotic saddle of what was the chaotic attractor at $g > 0.31$ probably survives in the invariant subspace. If so, in this intermittency, there are three invariant sets in the invariant subspace.

In this paper, we showed only the case of $N = 16$. We can, however, easily find the same intermittent behavior in other neuron numbers. In the limit of a continuous space ($N \to \infty$), the gap junction coupling term of our model, $g(V_{i+1} + V_{i-1} - 2V_i)$ is equivalent to $D\partial^2 V/\partial z^2$, where D is a diffusion coefficient defined by $\lim_{N\to\infty} g/N^2$, where z is a space variable and takes a scalar value. Therefore, if two network systems of sufficiently large neuron numbers N_1 and N_2 exhibit the same behaviors at g_1 and g_2 respectively, their coupling strengths scaled by neuron numbers are equal each other:

$$\frac{g_1}{N_1^2} \sim \frac{g_2}{N_2^2}. \tag{6}$$

We can roughly estimate a coupling strength at which a coupled system of 32 neurons exhibits the same in-out intermittency as the system of 16 neurons, using the above relation:

$$(\frac{32}{16})^2 0.255 = 1.02, \tag{7}$$

where 0.255 is the coupling strength at which the $N = 16$ system exhibits the in-out intermittency. In fact we found the same in-out intermittency at $g \sim 1.0$ in the case of

32 neurons. Validity of this estimation suggests that the continuous space limit is satisfied already at $N \geq 16$.

This network exhibits various behaviors, depending on the injected current and the coupling strength. We have found other interesting behaviors different from in-out intermittency, for example, chaotic itinerancy and on-off intermittency. We will discuss about the dynamical mechanism of these phenomena and the bifurcation structure of the network in the forthcoming papers.

---

[1] A. L. Hodgkin, The local electric changes associated with repetitive action in a nonmodulated axon, J. Physiol. 107, 165-181 (1948).

[2] B. Cauli, et al., Molecular and physiological diversity of cortical nonpyramidal cells, J. Neurosci. 17, 3894-3906 (1997).

[3] I. Tsuda, H. Fujii, S. Tadokoro, T. Yasuoka, Y. Yamaguti, Chaotic Itinerancy as a Mechanism of Irregular Changes between Synchronization and Desynchronization in a Neural Network, J. of Integrative Neuroscience 3, 159-182 (2004).

[4] H. Fujii and I. Tsuda, 'Neocortical gap junction-coupled interneuron systems may induce chaotic behavior itinerant among quasi-attractors exhibiting transient synchrony', Neurocomputing 58-60, 151-157 (2004).

[5] H. Fujii and I. Tsuda, Itinerant Dynamics of Class I^* Neurons Coupled by Gap Junctions. Lecture Notes in Computer Science, vol. 3146, 140-160. (Springer-Verlag, 2004)

[6] C. M. Gray, P. Koenig, A. K. Engel and W. O. Singer, Synchronization of Oscillatory Neuronal Responses in Cat Striate Cortex: Temporal Properties, Visual Neurosci. 8, 337-347 (1992).

[7] P. Ashwin, E. Cova, R. Tavakol, Transverse Instability for Non-normal Parameters, Nonliniarity 12, 563-577 (1999).

[8] N. Schweighofer, K. Doya, and M. Kawato, Electrophysiological properties of inferior olive neurons: A compartment model, J. Neurophysiol. 82, 804-817 (1999).

[9] J. Milnor, On the Concept of Attractor, Commun. Math. Phys. 99, 177-195 (1985).

[10] K. Ikeda, K. Otsuka and K. Matsumoto, Maxwell-bloch turbulence, Prog. Theor. Phys. Suppl. 99, 295-324 (1989).

[11] K. Kaneko, Clustering, Coding, Switching, Hierarchical Ordering, and Control in Network of

Chaotic Elements, Physica D 41, 137-172 (1990).

[12] I. Tsuda, Chaotic itinerancy as a dynamical basis of Hermeneutics in brain and mind, World Futures 32, 167-184 (1991).

[13] I. Tsuda, Dynamic Link Memories - Chaotic Memory Map in Nonequilibrium Neural Networks, Neural Networks 5, 313-326 (1992).

[14] K. Kaneko and I. Tsuda, eds. Chaotic Itinerancy, Focuas issue in Chaos 13, 926-1164 (2003).

[15] I. Shimada and T. Nagashima, A Numerical Approach to Ergodic Problem of Dissipative Dynamical Systems, Prog. Theor. Phys. 68, 349-358 (1979).

[16] G. Benettin, L. Galgani, A. Giorsilli and J. M. Strelcyn, Lyapunov Characteristic Exponents for Smooth Dynamical Systems and for Hamiltonian Systems; A Method for Computing All of Them Part 1: Theory, Mecannica 15, 9-20 (1980); Lyapunov Characteristic Exponents for Smooth Dynamical Systems and for Hamiltonian Systems; A Method for Computing All of Them Part 2: Numerical Application, Mecannica 15, 21-30 (1980). 15, 21-30 (1980).

[17] C. Grebogi, E. Otto and J. A. Yorke, Chaotic Attractors in Crisis, Phys. Rev. Lett. 48, 1507 (1982).